Lasers in Medical Science (2020) 35:1509–1518
https://doi.org/10.1007/s10103-019-02941-y

ORIGINAL ARTICLE

Attenuation of the inflammatory response and polarization of macrophages by photobiomodulation

Kun Li[1] · Zhuowen Liang[1] · Jiawei Zhang[1] · Xiaoshuang Zuo[1] · Jiakai Sun[1] · Qiao Zheng[1] · Jiwei Song[1] · Tan Ding[1] · Xueyu Hu[1] · Zhe Wang[1]

Received: 13 February 2019 / Accepted: 22 December 2019 / Published online: 17 February 2020
© Springer-Verlag London Ltd., part of Springer Nature 2020

Abstract

In spinal cord injury (SCI), inflammation is a major mediator of damage and loss of function and is regulated primarily by the bone marrow-derived macrophages (BMDMs). Photobiomodulation (PBM) or low-level light stimulation is known to have anti-inflammatory effects and has previously been used in the treatment of SCI, although its precise cellular mechanisms remain unclear. In the present study, the effect of PBM at 810 nm on classically activated BMDMs was evaluated to investigate the mechanisms underlying its anti-inflammatory effects. BMDMs were cultured and irradiated (810 nm, 2 mW/cm^2) following stimulation with lipopolysaccharide and interferon-γ. CCK-8 assay, 2′,7′-dichlorofluorescein diacetate assay, and ELISA and western blot analysis were performed to measure cell viability, reactive oxygen species production, and inflammatory marker production, respectively. PBM irradiation of classically activated macrophages significantly increased the cell viability and inhibited reactive oxygen species generation. PBM suppressed the expression of a marker of classically activated macrophages, inducible nitric oxide synthase; decreased the mRNA expression and secretion of pro-inflammatory cytokines, tumor necrosis factor alpha, and interleukin-1 beta; and increased the secretion of monocyte chemotactic protein 1. Exposure to PBM likewise significantly reduced the expression and phosphorylation of NF-κB p65 in classically activated BMDMs. Taken together, these results suggest that PBM can successfully modulate inflammation and polarization in classically activated BMDMs. The present study provides a theoretical basis to support wider clinical application of PBM in the treatment of SCI.

Keywords Photobiomodulation · Spinal cord injury · Macrophage · Polarization · Inflammation

Introduction

Spinal cord injury (SCI) typically occurs in two main stages. The acute stage is usually caused by direct trauma and cannot be reversed, while the second stage develops from acute injury which is characterized by factors such as excitotoxic damage, hemorrhage, ischemia, and a dramatic inflammatory response, which in turn leads to cell death and scar formation and finally cause permanent loss of moto function of patients [1]. Studies have found that the inflammatory response is essential to the second stage of SCI [2], and that macrophages are the most important participants in the inflammatory response [3–5]. Monocytes participating in SCI predominantly belong to two groups: bone marrow-derived macrophages (BMDMs) and specialized central nervous system (CNS)-resident microglia. The role of BMDMs appears to be more important than microglia during SCI, pathological process, as they occupy the center of the lesion site and secrete a large number of cytotoxic substances [6–8]. Macrophages can be polarized into either classically activated macrophages (M1 phenotype) with neurotoxicity or alternatively activated macrophages (M2 phenotype) with anti-inflammatory and prosthetic effects under different microenvironment [9]. Different from other tissue damage repair processes, during SCI, M1 cells continue to dominate in damage area, while there is only a transient increase in M2 cells, and the special polarization characteristics of macrophage in SCI pathological

Zhe Wang is corresponding author and Xueyu Hu is the co-corresponding author.

Kun Li, Zhuowen Liang and Jiawei Zhang are co-first author.

✉ Zhe Wang
wangzhe@fmmu.edu.cn

✉ Xueyu Hu
huxueyu@fmmu.edu.cn

[1] Xijing Orthopaedics Hospital, Fourth Military Medical University, Xi′an, Shaanxi, China

process exacerbate the difficulty of SCI injury repair [10–12]. Regulating the polarization of macrophages during SCI, inhibiting polarization into M1 cells and increasing polarization into M2 cells, can promote damage repair [13–16].

Photobiomodulation (PBM), also known as low-level light irradiation (LLLI), uses low doses of light from a near-infrared laser to achieve therapeutic effect and has been applied to treatments of various diseases [17]. PBM can significantly reduce the expression of inflammatory mediators, reduce pain and edema, and stimulate collagen remodeling [18–21]. Based on the above advantages, PBM has previously been used in spine transection and contusion animal models, with notable beneficial effects to reduce inflammation [22–26]. PBM has a significant effect on the infiltration and activation of macrophages/microglia and can downregulate the expression of pro-inflammatory factors such as interleukin 6 (IL-6), tumor necrosis factor alpha (TNF-α), and inducible nitric oxide synthase (iNOS) while upregulating the expression of interleukin 10 (IL-10). Our investigation has showed that PBM at 810 nm in a SCI rat model revealed that PBM had neuroprotective effects, promoted function recovery, and changed the polarization of macrophage at the site of spinal lesion, decreasing the proportion of M1 macrophages and increasing the number of M2 macrophages [26]. However, we did not distinguish between BMDMs and microglia in this previous experiment. It remains unclear whether PBM is effective on BMDMs, which play a vital role during SCI. Many studies have found that PBM can suppress the expression of M1 macrophage its pro-inflammatory mediators [27–31]. However, the experimental parameters in these studies, including energy density, total energy, and especially wavelength, were different from those of our studies. More importantly, most of these studies used macrophage cell lines. Due to the differences between immortalized cell lines and primary cells, and the unique microenvironment of the SCI lesions, previous studies may not have accurately inferred the effects of PBM on BMDMs during spinal cord injury. To determine the effect of PBM on M1-type BMDMs, the present study used PBM (810 nm) to treat on classically activated BMDMs and measured the effect of PBM on inflammatory markers and macrophage activation. This study will deepen our understanding of the molecular mechanisms underlying PBM treatment, particularly in the treatment effects of SCI, and promote clinical application of PBM in the treatment of spinal cord injury.

Methods

Differentiation and stimulation of macrophages

BMDMs were derived from bone marrow precursors of 6–8-week-old BALB/c mice as described by Meerpohl et al. [32]. All procedures were performed following the guidelines established by the Animal Care Ethics Committee of the Fourth Military Medical University, Xi'an, P.R. China. All necessary care was taken to minimize the suffering of the animal during sacrifice. Cells were seeded at 1×10^6 cells/mL of medium in 12-well cell culture plates. BMDMs cells were induced into M0-type macrophages by M-CSF conditioned medium (10% FBS, 1% penicillin streptomycin double antibody, DMEM high-sugar medium, 10 ng/mL M-CSF) for 7 days. Then M0-type macrophages were cultured with 100 ng/mL LPS (from *E. coli*, 0111.B4; Sigma Aldrich, USA) and 10 ng/mL IFN-gamma (from *E. coli*, PeproTech, USA) [33] at 37 °C with 5% CO_2 in a humid atmosphere for 24 h, which were induced into M1-type macrophages.

Photobiomodulation

A MW-GX-808 diode laser system was used for PBM (Lei Shi Optoelectronics Co., Ltd. Changchun, China). It employed a wavelength of 810 nm and 150 mW output power and had a 4.5 cm^2 light spot. An optic fiber and a collimating mirror were used to irradiate the cells immediately after stimulation. The fiber and collimating mirror were positioned above the irradiation plane at a distance appropriate for optimal expansion of the ray (approx. 5.5 cm). The power was measured using a Laser Mate power meter (Daheng optical, Shanghai, China).

M1 macrophages were randomly divided into four groups on the basis of treatment factor: control (ctrl), 0.4 J, 4 J, and 10 J groups. The number of cells was equal in each group. Wells of M1 macrophages were irradiated at 2 mw/cm^2 for 44 s (0.4 J), 440 s (4 J), and 1111 s (10 J) at 37 °C, 5% CO_2 incubator (Thermo Scientific, USA). During irradiation, the control plates were positioned in a covered box near the irradiated plate.

Immunofluorescence staining

The cells were transferred into confocal dish and washed with PBS three times, 5 min/time; the cells were fixed with paraformaldehyde for 15 min, permeabilized using 0.3% Triton X-100 for a total of 15 min, and blocked with 1% FBS at room temperature for 40 min. The samples were incubated at 4 °C overnight with rat anti-F4/80 or rabbit polyclonal anti-iNOS (both 1:400, Abcam, Cambridge, MA) or rat anti-CD86 or rabbit anti-CD206 (both 1:300, Abcam, Cambridge, MA). After the primary antibody was removed, the samples were washed with PBS three times, 5 min/time, followed by incubation in the dark at room temperature for 40 min with either Alexa Fluor 488-conjugated goat anti-rat secondary antibody or Alexa Fluor 594-conjugated donkey anti-rabbit secondary antibody (both 1:500, Absin, Shanghai, China).

Cell viability assay

Cell viability was determined using a Cell Counting Kit-8 (Dojindo, Japan) according to the manufacturer's instructions. Twenty-four hours after irradiation, cells were incubated with the CCK-8 agent and incubated at 37 °C in a humidified incubator containing 5% CO_2 for 4 h. The absorbance was measured at 450 nm using an automated microplate reader (Bio-Tek, USA).

ROS formation assay

The intracellular ROS levels were measured using 2,7-dichlorodihydrofluorescein diacetate (H_2DCF-DA; Nanjing Jiancheng Bioengineering Institute). After maturation of the BMDMs, the cells were seeded in a 96-well plate at a density of 10^4 cells/well and then irradiated as previously described. After irradiation, 20 μM DCF-DA was added to the macrophage medium, and the fluorescence of DCF was detected 2 h later using a fluorescent microplate reader (Bio-Tek, USA) at an excitation wavelength of 485 nm and an emission wavelength of 525 nm.

Reverse transcription quantitative real-time PCR

To determine the transcript levels of the genes being investigated, M0-type and M1-type RNA was isolated from the total cell lysate using the Total RNA Kit I 6 h after PBM treatment (Omega Bio-tek, USA) and was transcribed into cDNA using a reverse transcription kit (TaKaRa, Kyoto, Japan) according to the manufacturer's instructions. Real-time PCR was performed using a CFX96 Touch™ Real-Time PCR Detection System (Bio-Rad Laboratories, CA, USA) in conjunction with PrimeScript™ RT Master Mix (TaKaRa). The β-actin gene was used to normalize gene expression by parallel amplification and calculate the relative mRNA expression levels of the target genes. The PCR primer sequences are listed in Table 1.

Table 1 qRT-PCR primers used to detect TNF-α, iNOS, IL-1β and MCP-1

Gene		
TNF-α	Forward	5'-TTCAGGCAGGCAGTATCACTCATTG-3'
	Reverse	5'-GTGGTTTGTGAGTGTGAGGGTCTG-3'
iNOS	Forward	5'-ATCTTGGAGCGAGTTGTGGATTGTC-3'
	Reverse	5'-TTCAGGCAGGCAGTATCACTCATTG-3'
IL-1β	Forward	5'-TTCAGGCAGGCAGTATCACTCATTG-3'
	Reverse	5'-ACACCAGCAGGTTATCATCATCATCC-3'
MCP-1	Forward	5'-TTCAGGCAGGCAGTATCACTCATTG-3'
	Reverse	5'-TTCAGGCAGGCAGTATCACTCATTG-3

ELISA

ELISA was performed 24 h after treatment with PBM. The amount of secreted TNF-α protein was assessed in the culture supernatant using the TNF-α ELISA kit (BOSTER, Wuhan, China), according to the manufacturer's protocol. The amount of secreted IL-1β protein was similarly assessed in the culture supernatant using the IL-1β ELISA kit (BOSTER, Wuhan, China), according to the manufacturer's protocol. MCP-1 secretion was measured using the MCP-1 ELISA kit (InvivoGen, San Diego, USA). The absorbance of each well was measured at a wavelength of 450 nm using a conventional plate reader (Shanghai Spectrophotometer Co. Ltd., China).

Western blot analysis

Western blot analysis was performed 24 h after treatment with PBM. SDS–PAGE and immunoblotting were performed according to standard procedures. Briefly, cells were lysed in RIPA buffer on ice, and after separating the protein samples on 10% SDS polyacrylamide gels, total protein was transferred to 0.22 mm PVDF membranes (Millipore). The membranes were probed overnight with the antibodies, rabbit anti-iNOS (1:500, Santa Cruz, Texas, USA), rabbit anti-NF-κB p65 (1:1000, Cell Signaling Technology, USA), and rabbit anti-Phosphor-NF-κB p65 (1:1000, Cell Signaling Technology) at 4 °C, and the bound antibodies were tagged with a HRP-conjugated secondary antibody (A0216; Beyotime Biotechnology, China) at room temperature for 1 h. Use Trident femto Western HRP Substrate (GeneTex) to develop the membranes, which were imaged and analyzed using an Odyssey infrared imaging system (LICOR Bioscience). An anti-glyceraldehyde phosphate dehydrogenase (GAPDH, 1:1000, Abcam plc, Cambridge, UK) antibody was used as an internal control.

Statistical analysis

Image J pro-plus software (Media Cybernetics, USA) was used to analyze fluorescence intensity; Image J software (National Institutes of Health, Bethesda, MD) was used for the analysis of the bands. SPSS 19.0 (IBM Corp., USA) was used for statistical analysis. All experiments were performed at least in triplicate independently. Quantifiable data are expressed as mean values ± standard deviations (SD) of the mean. Statistical comparisons were made using one-way analysis of variance (ANOVA), and multiple comparisons between groups were performed using Turkey's test. Statistical significance was set at $*P < 0.05$, $**P < 0.01$, and $***P < 0.001$.

Results

Identification of macrophages

F4/80 is the marker of macrophage; iNOS is the marker of M1-type macrophages. The results from immunofluorescence showed that, after adding LPS and IFN-γ, the ratio of F4/80$^+$iNOS$^+$ macrophages in M1 group (86.3 ± 3.8%) was significantly higher than that in M0-type macrophages group (10.9 ± 2.1%) ($P < 0.01$). (Fig. 1a and b).

Effect of PBM on cell viability in classically activated BMDM

A CCK8 assay was used to determine if PBM treatment had any effect on the viability of classically activated BMDMs. A total of 4 J PBM-treated group has increased cell viability compared with that of the control group (Fig. 2a). Notably, the viability of classically activated macrophages in the 4 J PBM increased significantly from 1.000 ± 0.069 to 1.37 ± 0.216 ($P = 0.0207$). The 4 J group had a significantly higher cell viability than that of the 0.4 J group (from 1.017 ± 0.027 to 1.37 ± 0.216, $P = 0.0264$) and the 10 J group (from 0.879 ± 0.079 to 1.37 ± 0.216, $P = 0.0043$).

The effect of PBM on intracellular ROS levels in classically activated BMDMs

A DCF-DA assay was used to measure the intracellular ROS generation of classically activated BMDMs following PBM treatment. At 2 h after PBM treatment, the DCF fluorescence intensity of the 10 J group increased significantly compared with that of the control group (from 0.571 ± 0.051 to 0.867 ± 0.090, $P < 0.001$), suggesting that ROS generation in the 10 J group was significantly increased compared with that of the control group (LPS + INF-γ stimulated) (Fig. 2b). However, the 0.4 and 10 J groups did not show any significant changes 2 h after PBM treatment. The DCF fluorescence intensity of the 10 J group also exceeded that of the 0.4 J (0.582 ± 0.094 vs 0.867 ± 0.090, $P < 0.001$) and 4 J groups (0.643 ± 0.089 vs 0.867 ± 0.090, $P < 0.001$). At 24 h post-irradiation, the DCF fluorescence intensity of the 4 J group was significantly decreased compared with that of the control group (from 0.481 ± 0.076 to 0.264 ± 0.048 $P = 0.0296$), suggesting a noticeable decrease in ROS activity in these groups. The DCF

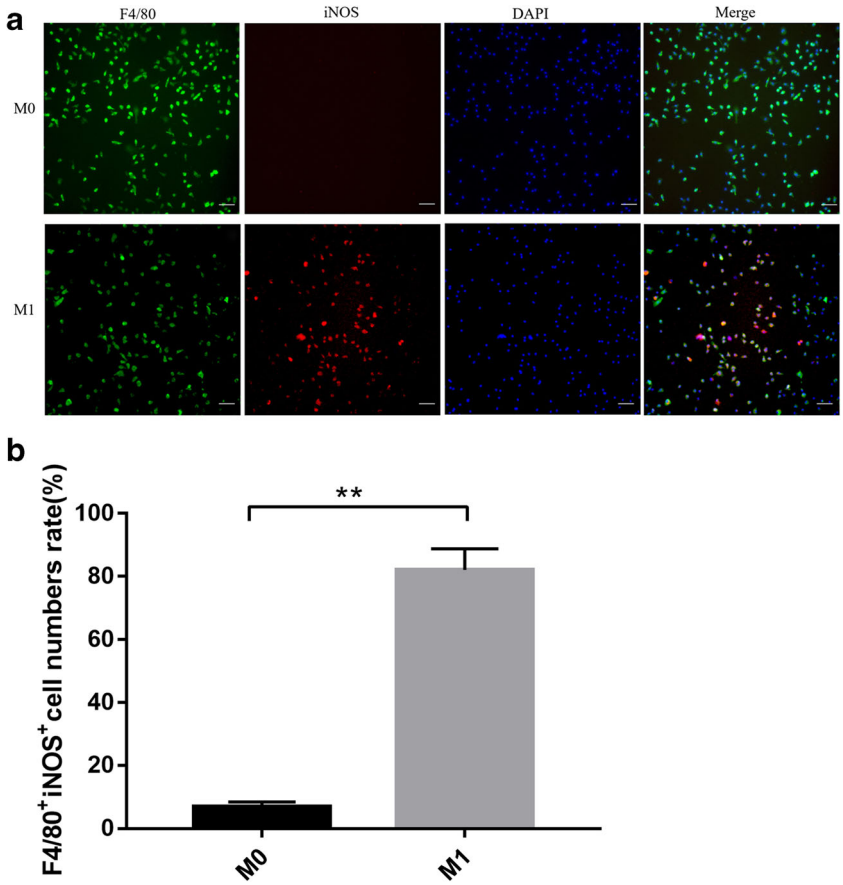

Fig. 1 Identification of macrophages. **a** The upper panel, after stimulated by M-CSF, macrophages marker F4/80 was significantly expressed. The lower panel, M0 macrophages were induced by LPS + INF-γ for 24 h; M1 macrophages marker iNOS were significantly expressed. Bar, 200 μm. **b** The ratio of F4/80 + iNOS + cells in the M1 group was significantly improved compared with the M0 group. (**$P < 0.01$)

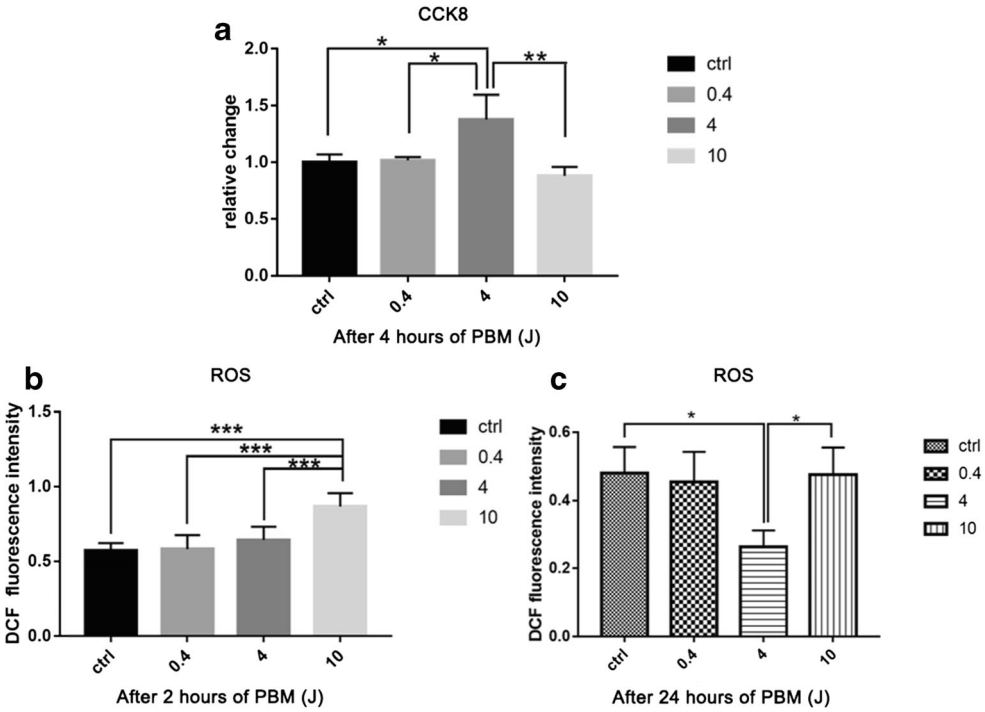

Fig. 2 Effect of phosphobiomodultion (PBM) on cell viability and ROS production. a 24 h after stimulation and irradiation, bone marrow-derived macrophages (BMDMs) were incubated with the indicated concentration of CCK-8 agent for 4 h. Cell viability is expressed as means ± SD (*$P < 0.05$, **$P < 0.01$ vs. control group, $n \geq 3$ independent experiments for each group). DCF fluorescence of the control (ctrl) and PBM (0.4 J, 4 J and 10 J) groups (**b**) 2 and (**c**) 24 h after PBM irradiation. The fluorescence results are expressed as means ± SD (*$P < 0.05$, **$P < 0.01$, and ***$P < 0.001$ vs. control group, $n \geq 3$ independent experiments for each group)

fluorescence intensity of the 10 J group was much higher than that of the 4 J group (from 0.476 ± 0.080 to 0.264 ± 0.048 $P = 0.0337$) (Fig. 2c).

Effect of PBM on the expression of cytokine and chemokine genes in classically activated BMDMs

RT-PCR was employed to determine the relative expression of relevant genes in M0 and M1 macrophages in response to 0.4, 4, and 10 J of PBM. Compared with M0 group, the expression of iNOS, IL-1β, TNF-α, and MCP-1 in the M1 group were significantly higher than M0 group ($P < 0.0001$). The results showed that M0 macrophages were successfully polarized into M1-type macrophages after being treated with LPS and interferon for 24 h (Fig. 3). There was no statistical difference of relative gene expression between M0 group and M0 + 0.4 J, M0 + 4 J, and M0 + 10 J groups.

The TNF-α mRNA expression in the 0.4 J and 4 J PBM groups decreased substantially compared with that of the control group (downregulated to 0.669 ± 0.192-fold of the control in the 0.4 J group and 0.647 ± 0.08-fold of the control in the 4 J group, $P = 0.032$ and 0.023, respectively; Fig. 4a). Although the relative TNF-α mRNA expression of the 10 J PBM group decreased compared with that of the control group, the difference was not statistically significant (Fig. 4a). We also investigated the impact of PBM on the classic polarization marker iNOS. After irradiation, the mRNA levels of iNOS significantly decreased in all PBM-treated groups. The relative mRNA expression of iNOS was downregulated to 0.714 ± 0.109-fold of the control in

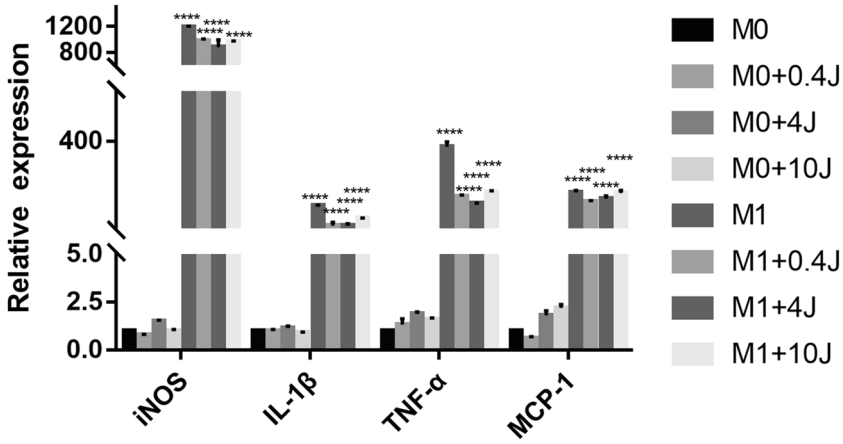

Fig. 3 RT-PCR was used to determine the expression of relevant genes in M0 and M1 macrophages in response to 0.4, 4, and 10 J of PBM. The expression of iNOS, IL-1β, TNF-α, and MCP-1 in the M1 group was significantly higher than M0 group ($P < 0.0001$). There was no statistical difference of relative gene expression between M0 group and M0 + 0.4 J, M0 + 4 J, and M0 + 10 J groups

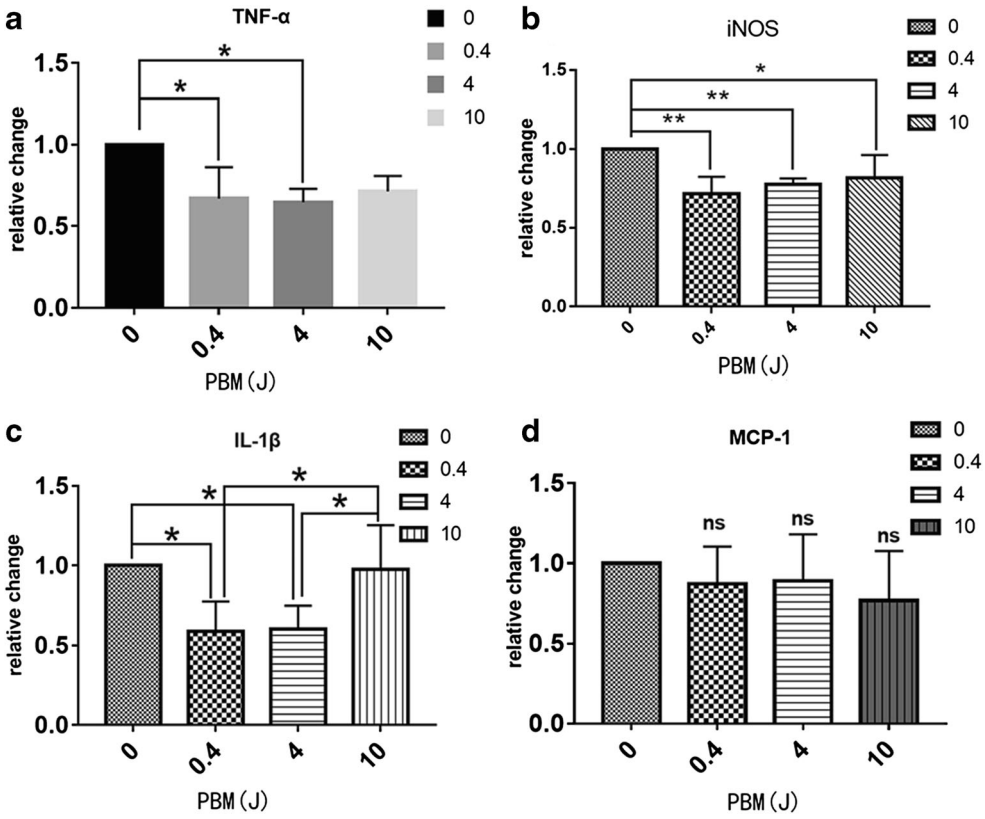

Fig. 4 Effect of PBM on the mRNA expression of classically activated macrophage cytokine-chemokine signals. Quantitative analysis of mRNA expression of tumor TNF-α (**a**), iNOS (**b**), IL-1β (**c**), and MCP-1 (**d**). The relative mRNA expression levels are expressed as the means ± SD (*$P < 0.05$, **$P < 0.01$ vs. control group, n ≥ 3 independent experiments for each group). *TNF-α* tumor necrosis factor alpha; *iNOS* inducible nitric oxide synthase; *IL-1β* interleukin 1 beta; *MCP-1* monocyte chemotactic protein 1

the 0.4 J group, 0.774 ± 0.039 in the 4 J group, and 0.818 ± 0.144 in the 10 J group ($P = 0.001$, 0.007, and 0.031, respectively). However, no significant differences were detected among the PBM groups (Fig. 4b). The relative IL-1β mRNA levels similarly significantly decreased compared to the control in the 0.4 J (reduced to 0.587 ± 0.189-fold of the control, $P = 0.012$) and 4 J PBM groups (reduced to 0.605 ± 0.145-fold of control, $P = 0.017$), but no statistically significant difference was detected between the control and the 10 J PBM group. Among the PBM groups, the IL-1β mRNA expression was significantly higher in the 10 J group than in the 0.4 J (0.714 ± 0.109 vs 0.975 ± 0.278, $P = 0.019$) and 4 J groups (0.774 ± 0.039 vs 0.975 ± 0.278, $P = 0.026$) (Fig. 4c). We also investigated the mRNA levels of MCP-1 (CCL2), but no statistically significant differences were observed between the groups (Fig. 4d).

Impact of PBM on the polarization state of classically activated BMDMs

To study the effects of PBM on the polarization state of classically activated macrophages, we measured the protein levels of the polarization markers iNOS by western blotting and TNF-α, IL-1β, and MCP-1 by ELISA. According to western blot analysis, the expression of iNOS protein at 24 h after PBM treatment decreased from 1.000 ± 0.077 to 0.550 ± 0.230-fold in the 0.4 J group compared to that of the control ($P = 0.025$). The iNOS expression in the 4 J group similarly decreased, from 1.000 ± 0.077 to 0.214 ± 0.01-fold ($P = 0.001$). In the 10 J group, there was a slight decrease in iNOS expression of 0.716 ± 0173-fold relative to the control, but this was not statistically significant ($P = 0.169$) (Fig. 5a and b).

ELISA assays were performed to measure the amount of secreted TNF-α, IL-1β, and MCP-1. The mean supernatant levels of TNF-α in the 4 J PBM group decreased significantly compared to that of the control group (from 270.480 ± 26.831 to 209.365 ± 5.600 pg/mL, $P = 0.013$) (Fig. 5c). A similar pattern was observed in the 10 J PBM group (from 70.480 ± 26.831 to 201.829 ± 18.070 pg/mL, $P = 0.0064$). However, the mean supernatant level of TNF-α in the 0.4 J PBM group did not change compared to that of the control group (270.480 ± 26.831 vs. 272.921 ± 13.507 pg/mL, $P = 0.999$). Among the PBM groups, the secretion of TNF-α in the 0.4 J group was significantly higher than that of the 4 J and 10 J groups ($p = 0.01$ and 0.005, respectively; Fig. 5c). The mean supernatant levels of IL-1β (Fig. 5d) in the 0.4 J PBM group were significantly lower than that of the control group (49.406 ± 11.304 vs. 78.362 ± 2.760 pg/mL, $P = 0.0054$). The mean supernatant level of IL-1β in the 4 J PBM group similarly decreased compared to that of the control (from 78.362 ± 2.760 to 55.156 ± 7.390 pg/mL, $P = 0.019$). In the 10 J group, the secretion of IL-1β was not significantly different to that of the control. In the 0.4 J group, MCP-1 secretion increased to 141.502 ±

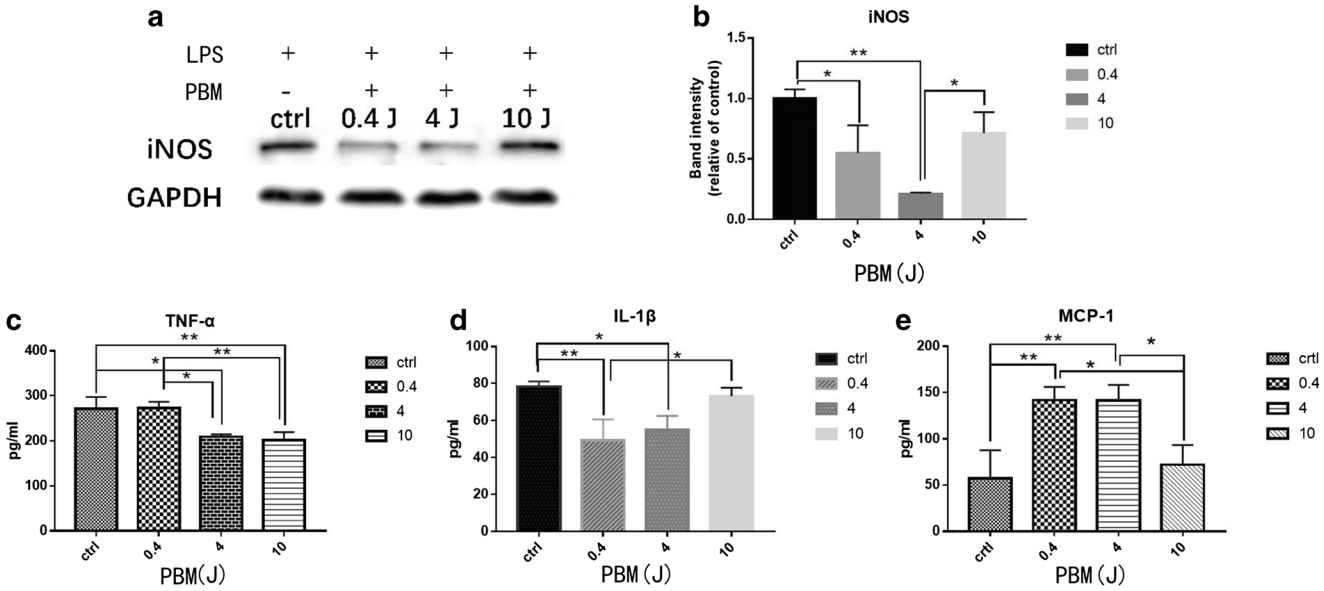

Fig. 5 Effect of PBM on the expression of iNOS, TNF-α, IL-1β, and MCP-1 proteins. Relative expression of iNOS (**a** and **b**), TNF-α (**c**), IL-1β (**d**), and MCP-1 (**e**) in the control and PBM groups. GAPDH was used as a loading control. The protein expression levels are expressed as mean ± SD (*$P < 0.05$, **$P < 0.01$ vs. control group, n ≥ 3 independent experiments for each group)

14.426 from 57.274 ± 30.503 pg/mL in the control group ($P = 0.006$). In the 10 J group, MCP-1 secretion increased to 141.406 ± 16.920 pg/mL (P = 0.006). MCP-1 also increased slightly to 71.990 ± 21.350 pg/mL in the 10 J group, but there was no statistically significant difference with respect to the control ($p = 0.839$). The secretion of MCP-1 in the 0.4 J and 4 J groups significantly exceeded that of the 10 J group ($P = 0.019$ and 0.019, respectively; Fig. 5e).

Inhibition of NF-κB p65 expression and phosphorylation by PBM in classically activated macrophages

We further investigated the impact of PBM on the expression and phosphorylation of the classically activated macrophage polarization transcription factor NF-κB p65. Compared with that of the control group, NF-κB p65 expression decreased in

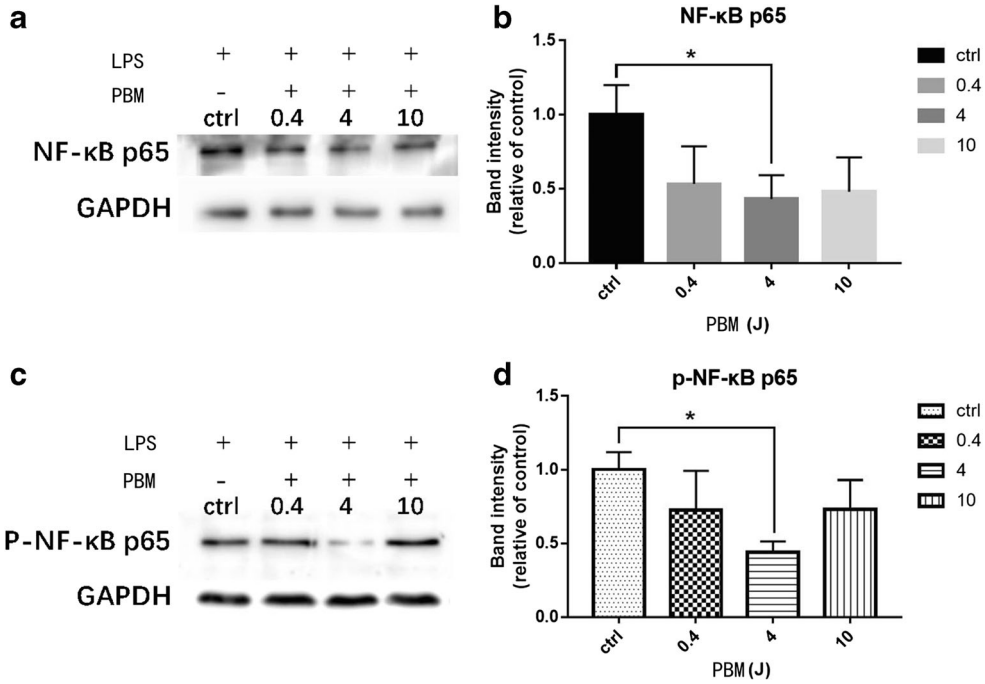

Fig. 6 Effect of PBM on the expression and phosphorylation of NF-κB p65. (**a** and **b**) Relative expression of NF-κB p65 in the control and PBM groups (**c** and **d**) and relative abundance of phosphorylated p-NF-κB p65 in the control and PBM groups. GAPDH was used as a loading control. The protein expression levels are expressed as means ± SD (*$P < 0.05$, **$P < 0.01$ vs. control group, n ≥ 3 independent experiments for each group)

the irradiated groups. Specifically, in the 4 J group, the expression decreased from 1.000 ± 0.201 to 0.431 ± 0.161-fold, $P = 0.047$. In the 10 J group the expression of NF-κB p65 also decreased slightly compared to that of the control (from 1.000 ± 0.200 to 0.480 ± 0.233-fold, $P = 0.070$). The expression of NF-κB p65 in the 0.4 J PBM group was not significantly different to that of the control ($P = 0.107$). There were no statistically significant differences in NF-κB p65 expression between PBM treatment groups (Fig. 6a and b). Next, we examined the influence of 810 nm irradiation on the phosphorylation of NF-κB p65 (p-NF-κB p65). The relative abundance of p-NF-κB p65 decreased significantly in the 4 J group (from 1.00 ± 0.119 to 0.441 ± 0.072-fold, $P = 0.021$) compared with that of the control. We also observed a slight reduction in p-NF-κB p65 in the 0.4 J and 10 J groups relative to that of the control, but this difference was not statistically significant ($P = 0.316$, $P = 0.328$) (Fig. 6c and d).

Discussion

In the present study, we measured the effects of PBM (810 nm) on classically activated BMDMs and observed that PBM treatment inhibits polarization; suppresses the expression and secretion of TNF-α, iNOS, and IL-1β; and also increases the secretion of MCP-1.The PBM of 0.4, 4, and 10 J had a slight effect on the function of M0 macrophages, but there was no statistical significance [34]; 4 J PBM has an inhibitory effect on the expression of inflammatory factors in M1 macrophages, and the results are much different from those in the M0 group, indicating that PBM has little effect on normal macrophages without LPS and IFN-γ treatment. PBM also significantly downregulated the expression and phosphorylation of NF-κB p65. Our results indicate that PBM treatment of BMDMs at a power of 2 mW/cm^2 for 440 s (4 J) can increase cell viability and inhibit ROS production in classically activated BMDMs.

iNOS is a molecular and cellular marker of classically activated macrophages, which is involved in mediating the inflammatory response, and induces apoptosis following SCI. It is also a marker for NO activity, which is considered to be neurotoxic under conditions of cerebral ischemia [35]. Our findings indicate that PBM can significantly reduce the expression as well as secretion of iNOS by M1 BMDMs. Gavis et al. found that 780 nm LLLI had little effect on iNOS mRNA expression but increased the production of NO [27]. Silva et al. used two wavelengths (660 nm and 808 nm) with a relatively high dose of energy (11–214 J/cm^2) to irradiate RAW 264.7 cells and found an increase in iNOS expression [36]. Fernandes et al. found that both 660 and 780 nm (660 nm, 15 mW, 7.5 J/cm^2, 20 s, and 780 nm, 70 mW, 2.6 J/cm^2, 1.5 s) laser treatment reduced the expression of iNOS in J774 cells. However, the different parameters (wavelength, power intensities) and cell type (RAW 264.7 vs. BMDM) used in these studies may explain the divergent observations. This finding highlights the fact that choosing the right parameters would be critical for PBM-based treatment of SCI.

TNF-α is a crucial cytokine produced by classically activated macrophages that hinders the process of wound repair. In the present study, PBM significantly downregulated the mRNA levels of TNF-α at 4 h post-irradiation and the secretion of TNF-α remained suppressed at 24 h after irradiation. These results are consistent with those of previous studies, further corroborating the fact that PBM treatment can inhibit the secretion of TNF-α [27, 30, 31]. The effect of laser irradiation on IL-1β, an important pro-inflammatory cytokine, has been extensively studied [27, 31]. Our findings confirmed the results of previous studies that a variety of wavelength/power settings of lasers can reduce the secretion of IL-1β by M1 macrophages.

Investigation of the effect of PBM on MCP-1 revealed an increase in secretion at 24 h. However, these changes may be time-dependent because at 4 h, there was no expression of MCP-1. As an important pro-inflammatory chemokine, the impact of PBM on the secretion of MCP-1 has also been well studied. Gavish et al. found that 780 nm, 2.2 J/cm^2 LLLI treatment reduced the LPS-induced secretion of macrophage MCP-1 by 17 ± 5% (0.1 mg LPS) and 13 ± 5% (1 mg/mL LPS) at 12 h, compared with that of non-irradiated cells. However, Leden et al. found that 808 nm irradiation at 0.2 J/cm^2 significantly increased MCP-1 secretion in LPS-induced microglia [27]. These somewhat contradictory findings suggest that different laser irradiation parameters may have widely varying effects on MCP-1 secretion. MCP-1 may also play an anti-inflammatory role during macrophage polarization and SCI. Sierra-Filardi et al. showed that MCP-1/CCR2 influences macrophage polarization by enhancing LPS-induced IL-10 secretion and MCP-1 blockage led to the expression of M1-associated genes and cytokines [37]. Kwon et al. found that MCP-1 plays a vital role in the neuron-macrophage interaction, and upregulation of MCP-1 promoted sensory axon regeneration [38]. Taken together, these findings suggest that the role of laser irradiation in promoting MCP-1 secretion may contribute to nerve injury repair. However, the precise nature of this interaction requires further experimental evidence.

The early signaling events that take place in mammalian cells upon PBM include a burst of reactive oxygen species (ROS) production [39]. Leden et al. studied the impact of 808 nm PBM on ROS generation by microglia and found that 2 h after PBM treatment at 0.2, 4, 10, and 30 J/cm^2, the generation of ROS in the LPS group was significantly increased compared with that of the control group (without irradiation and LPS stimulation) while, at 24 h after irradiation, ROS generation only increased in the 10 and 30 J/cm^2 groups [31]. However, the differences between the LPS stimulated

group and the irradiated groups were not investigated. Our results suggest that the effect of PBM on ROS generation in classically activated macrophages may be dose- and time-dependent as 2 h after irradiation ROS generation in the 10 J group was significantly increased compared with the control group. However, the 0.4 and 10 J groups did not show any significant changes in ROS levels up till 24 h after PBM irradiation; then, there was a noticeable reduction in ROS production.

Macrophage polarization is influenced by a variety of transcription factors, and NF-κB p65 and its phosphorylated form are considered as the classical transcription factors for the M1 phenotype [40]. Changes in ROS levels are highly correlated with NF-κB activation [41–43]. To further explore the related mechanisms, we investigated the effect of PBM on the classical macrophage polarization transcription factor NF-κB p65. We observed significantly decreased NF-κB p65 expression in the 4 and 10 J PBM groups. We also found that the 4 J PBM group had reduced levels of phospho-NF-κB p65 compared to that of the control. These findings suggest that 810 nm PBM may suppress the polarization of classically activated macrophages by influencing the activity of transcription factor NF-κB p65. However, the mechanism of macrophage polarization is complex, and the specific mechanism by which PBM may regulate polarization requires further investigation.

Conclusion

In conclusion, we found that PBM (810 nm) can directly act on classically activated BMDMs, inhibit polarization, increase cell viability, suppress ROS generation, and increase MCP-1 secretion. Furthermore, PBM also suppressed the expression and secretion of TNF-α, iNOS, and IL-1β. PBM can also significantly decrease the expression and phosphorylation of NF-κB p65. To the best of our knowledge, this study is the first to determine the effect of PBM on M1 BMDMs. The findings of this study can form a basis for the development of a foundation for PBM-based treatment strategies for SCI in the future.

Acknowledgments We thank Xi'an laser tech medical technology company LTD for providing the PBM device. The authors also wish to thank Prof. Jielai Xia from AFMU, China, for editing this manuscript.

Funding information This work is supported by grants from the National Natural Science Foundation of China (No. 81572151) and Key Science and Technology Program in Social Development of Shaanxi Province (2016SF-143).

Compliance with ethical standards

Conflict of interest The authors declare that they have no conflict of interest.

Ethics approval All the procedures that required the use of mice were performed following the guidelines established by the Animal Care Ethics Committee of the Fourth Military Medical University, Xi'an, P.R. China.

References

1. Oyinbo CA (2011) Secondary injury mechanisms in traumatic spinal cord injury: a nugget of this multiply cascade. Acta Neurobiol Exp 71(2):281–299
2. Faden AI, Wu J, Stoica BA et al (2016) Progressive inflammation-mediated neurodegeneration after traumatic brain or spinal cord injury. Br J Pharmacol 173(4):681–691
3. Horn KP, Busch SA, Hawthorne AL et al (2008) Another barrier to regeneration in the CNS: activated macrophages induce extensive retraction of dystrophic axons through direct physical interactions. J Neurosci 28(38):9330–9341
4. Busch SA, Horn KP, Silver DJ et al (2009) Overcoming macrophage-mediated axonal dieback following CNS injury. J Neurosci 29(32):9967–9976
5. Busch SA, Hamilton J, Horn KP et al (2011) Multipotent adult progenitor cells prevent macrophage-mediated axonal dieback and promote regrowth after spinal cord injury. J Neurosci 31(3):944–953
6. Nordendiana M, Fawtimothy D, Mckimdaniel B et al (2018) Bone marrow-derived monocytes drive the inflammatory microenvironment in local and remote regions after thoracic spinal cord injury. J Neurotrauma 2019,36(6):1–37
7. Greenhalgh AD, David S (2014) Differences in the phagocytic response of microglia and peripheral macrophages after spinal cord injury and its effects on cell death. J Neurosci 34(18):6316–6322
8. Evans TA, Barkauskas DS, Myers JT et al (2014) High-resolution intravital imaging reveals that blood-derived macrophages but not resident microglia facilitate secondary axonal dieback in traumatic spinal cord injury. Exp Neurol 254(4):109–120
9. Mosser DM, Edwards JP (2008) Exploring the full spectrum of macrophage activation. Nat Rev Immunol 8(12):958–969
10. Kigerl KA, Gensel JC, Ankeny DP et al (2009) Identification of two distinct macrophage subsets with divergent effects causing either neurotoxicity or regeneration in the injured mouse spinal cord. J Neurosci 29(43):13435–13444
11. Ren Y, Young W (2013) Managing inflammation after spinal cord injury through manipulation of macrophage function. Neural Plast 2013:945034
12. Samuel D, Antje K (2011) Repertoire of microglial and macrophage responses after spinal cord injury. Nat Rev Neurosci 12(7):388–399
13. Guerrero AR, Uchida K, Nakajima H et al (2012) Blockade of interleukin-6 signaling inhibits the classic pathway and promotes an alternative pathway of macrophage activation after spinal cord injury in mice. J Neuroinflammation 9(1):40
14. Li F, Cheng B, Cheng J et al (2015) CCR5 blockade promotes M2 macrophage activation and improves locomotor recovery after spinal cord injury in mice. Inflammation 38(1):126–133
15. Ji XC, Dang YY, Gao HY et al (2015) Local injection of Lenti–BDNF at the lesion site promotes M2 macrophage polarization and inhibits inflammatory response after spinal cord injury in mice. Cell Mol Neurobiol 35(6):881–890
16. Zhang Q, Bian G, Chen P et al (2014) Aldose reductase regulates microglia/macrophages polarization through the cAMP response element-binding protein after spinal cord injury in mice. Mol Neurobiol 53(1):662–676
17. T D, SK S, YY H et al (2012) The nuts and bolts of low-level laser (light) therapy.%A Chung H. Ann Biomed Eng 40(2):516–533

18. Manstein D, Laubach H, Watanabe K et al (2008) Selective cryolysis: a novel method of non-invasive fat removal. Lasers Surg Med 40(9):595–604
19. Jori G, Fabris C, Soncin M et al (2010) Photodynamic therapy in the treatment of microbial infections: basic principles and perspective applications. Lasers Surg Med 38(5):468–481
20. Jimenez JJ, Wikramanayake TC, Bergfeld W et al (2014) Efficacy and safety of a low-level laser device in the treatment of male and female pattern hair loss: a multicenter, randomized, sham device-controlled, double-blind study. Am J Clin Dermatol 15(2):115–127
21. Lívia A, Moretti AIS, Abrah OTB et al (2012) Low-level laser therapy (808 nm) reduces inflammatory response and oxidative stress in rat tibialis anterior muscle after cryolesion. Lasers Surg Med 44(9):726–735
22. Byrnes KR, Waynant RW, Ilev IK et al (2005) Light promotes regeneration and functional recovery and alters the immune response after spinal cord injury. Lasers Surg Med 36(3):171–185
23. Wu X, Dmitriev AE, Cardoso MJ et al (2009) 810 nm wavelength light: an effective therapy for transected or contused rat spinal cord. Lasers Surg Med 41(1):36–41
24. Hu D, Zhu S, Potas JR (2016) Red LED photobiomodulation reduces pain hypersensitivity and improves sensorimotor function following mild T10 hemicontusion spinal cord injury. J Neuroinflammation 13(1):200
25. Hu D, Zhu S, Potas JR (2016) Red LED photobiomodulation reduces pain hypersensitivity and improves sensorimotor function following mild T10 hemicontusion spinal cord injury. J Neuroinflammation 13(1):200
26. Song JW, Li K, Liang ZW et al (2017) Low-level laser facilitates alternatively activated macrophage/microglia polarization and promotes functional recovery after crush spinal cord injury in rats. Sci Rep 7(1):620
27. Gavish L, Perez LS, Reissman P et al (2008) Irradiation with 780 nm diode laser attenuates inflammatory cytokines while upregulating nitric oxide in LPS-stimulated macrophages: implications for the prevention of aneurysm progression. Lasers Surg Med 40(5):371–378
28. Souza NHC, Marcondes PT, Albertini R et al (2014) Low-level laser therapy suppresses the oxidative stress-induced glucocorticoids resistance in U937 cells: relevance to cytokine secretion and histone deacetylase in alveolar macrophages. J Photochem Photobiol B Biol 130(1):327–336
29. Ki Bum A, Seok-Seong K, Ok-Jin P et al (2014) Irradiation by gallium-aluminum-arsenate diode laser enhances the induction of nitric oxide by Porphyromonas gingivalis in RAW 264.7 cells. J Periodontol 85(9):1259–1265
30. Fernandes KPS, Souza NHC, Mesquita-Ferrari RA et al (2015) Photobiomodulation with 660-nm and 780-nm laser on activated J774 macrophage-like cells: effect on M1 inflammatory markers. J Photochem Photobiol B Biol 153:344–351
31. Leden REV, Cooney SJ, Ferrara TM et al (2013) 808?nm wavelength light induces a dose-dependent alteration in microglial polarization and resultant microglial induced neurite growth. Lasers Surg Med 45(4):253–263
32. Meerpohl HG, Lohmann-Matthes ML, Fischer H (2010) Studies on the activation of mouse bone marrow-derived macrophages by the macrophage cytotoxicity factor (MCF). Eur J Immunol 6(3):213–217
33. Kigerl KA, Gensel JC, Ankeny DP et al (2009) Identification of two distinct macrophage subsets with divergent effects causing either neurotoxicity or regeneration in the injured mouse spinal cord. J Neurosci 29(43):13435–13444
34. Hamblin MR, Huang YY, Heiskanen V (2019) Non-mammalian hosts and photobiomodulation: do all life-forms respond to light? 95(1):126–Photochem Photobiol, 139
35. Leung MCP, Lo SCL, Siu FKW et al (2010) Treatment of experimentally induced transient cerebral ischemia with low energy laser inhibits nitric oxide synthase activity and up-regulates the expression of transforming growth factor-beta 1. Lasers Surg Med 31(4): 283–288
36. Silva IHM, Andrade SCD, Fonsêca DDD et al (2016) Increase in the nitric oxide release without changes in cell viability of macrophages after laser therapy with 660 and 808 nm lasers. Lasers Med Sci 31(9):1855–1862
37. Elena SF, Concha N, Angeles DS et al (2014) CCL2 shapes macrophage polarization by GM-CSF and M-CSF: identification of CCL2/CCR2-dependent gene expression profile. J Immunol 192(8):3858–3867
38. Jung KM, Hae Young S, Yuexian C et al (2015) CCL2 mediates neuron-macrophage interactions to drive proregenerative macrophage activation following preconditioning injury. J Neurosci 35(48):15934–15947
39. Alexandratou E, Yova D, Handris P et al (2002) Human fibroblast alterations induced by low power laser irradiation at the single cell level using confocal microscopy. Photochem Photobiol Sci 1(8): 547–552
40. Hume DA (2015) The many alternative faces of macrophage activation. Front Immunol 6:1–10
41. Yu XJ, Zhang DM, Jia LL et al (2015) Inhibition of NF-κB activity in the hypothalamic paraventricular nucleus attenuates hypertension and cardiac hypertrophy by modulating cytokines and attenuating oxidative stress. Toxicol Appl Pharmacol 284(3):315–322
42. Jurk D, Wilson CL, Passos JF et al (2014) Chronic inflammation induces telomere dysfunction and accelerates ageing in mice. Nat Commun 5(1):4172
43. Chung IS, Kim JA, Kim JA et al (2013) Reactive oxygen species by isoflurane mediates inhibition of nuclear factor κB activation in lipopolysaccharide-induced acute inflammation of the lung. Anesth Analg 116(2):327–335

Publisher's note Springer Nature remains neutral with regard to jurisdictional claims in published maps and institutional affiliations.